Sulfur-enhanced reductive bioprocessing of cobalt-bearing materials for base metals recovery

Araujo Santos, Ana Laura; Dybowska, Agnieszka; Schofield, Paul; Herrington, Richard; Johnson, Barrie

Hydrometallurgy

DOI:
10.1016/j.hydromet.2020.105396

Published: 01/08/2020

Peer reviewed version

Sulfur-enhanced Reductive Bioprocessing of Cobalt-bearing Materials for Base Metals Recovery

Ana Laura Santos[1*], Agnieszka Dybowska[2], Paul F. Schofield[2], Richard J. Herrington[2] and D. Barrie Johnson[1]

[1]School of Natural Sciences, Bangor University, Bangor, LL57 2UW, UK

[2]Department of Earth Sciences, Natural History Museum, London, SW7 5BD, UK

*Corresponding author; ana.santos@bangor.ac.uk; Tel. +44 01248 382832

Keywords: acidophilic bacteria, cobalt, limonitic laterite, nickel, ore processing residues, reductive bioleaching

Abstract

The abundance of limonitic laterite ores in tropical and sub-tropical areas represents a large, and mostly unexploited, cobalt resource. Bioprocessing oxidised ores, and also waste materials such as tailings and processing residues, using acidophilic microorganisms to catalyse the reductive dissolution of iron and manganese minerals, is an environmentally benign alternative approach of extracting valuable base metals associated with these deposits. This work describes results from laboratory-scale experiments in which five cobalt-bearing materials, three primary limonitic laterite ores and two processing residues (filter dust and slag), all sourced from mines and a processing plant in Greece, were bioleached under reducing conditions by a consortium of acidophilic bacteria (using elemental sulfur as electron donor) in stirred tank bioreactors at pH 1.5 and 35ºC. Whilst the target metal, cobalt, was successfully bioleached from all five materials (40 - 50% within 30 days) the extraction of some other metals was more variable (e.g. between 2 and 48% of iron). Concentrations of soluble cobalt were highly correlated, in most cases, with those of manganese, correlating with the finding that cobalt was primarily deported in manganese (IV) minerals. Acid consumption also differed greatly between mineral samples, ranging between 3 and 67 moles H_2SO_4 g^{-1} cobalt extracted. Comprehensive mineralogical analysis of the three limonitic samples before and after bioprocessing revealed significant variations between the ores, and demonstrated that elemental and mineralogical variabilities can greatly impact their amenability for reductive bioleaching.

1. Introduction

The global demand for cobalt has greatly accelerated over the past 30 years, reflecting its increased use as an essential constituent of high technology materials, such as rechargeable batteries, superalloys and catalysts. Cobalt occurs in similar abundance to many other base metals such as copper and zinc in the earth's crust, though rarely in concentrations and amounts that have made it economically viable to be mined as a primary resource (Roberts and Gunn, 2014). In 2011, the European Union identified cobalt as a critical raw material, being fundamental to industry and essential for enabling technological development, and requiring reliable and sustainable supply. The Democratic Republic of Congo is the world's leading source of mined cobalt, accounting for approximately 70% of global cobalt production, and China is the world's leading consumer, with over 80% being used to produce rechargeable batteries (US Geological Survey, 2020). With the exception of the Bou Azzer cobalt mine in Morocco, cobalt is obtained as a secondary product of copper and nickel (from sulfide ores) and nickel (from lateritic ores) production (Roberts and Gunn, 2014).

Laterites are iron-rich deposits mostly found in tropical and subtropical areas. They are formed during the pervasive weathering of surface-located ultramafic rock leading to oxidation and precipitation of iron and enrichment of residual elements such as nickel and cobalt. The limonite layer of a laterite deposit typically contains 40 - 60% goethite (FeO·OH) along with 0.8 - 1.5% nickel and 0.05 - 0.2% cobalt (Dalvi et al., 2004). Nickel in limonite is typically associated with iron (III) minerals whereas cobalt is associated with manganese (IV) minerals, such as asbolane ($(Ni,Co)_xMn(O,OH)_4 \cdot nH_2O$) (Lambiv Dzemua et al., 2013). Although, 60% of the world's nickel production currently derives from sulfide ores, lateritic ores account for 70% of global nickel reserves (Dalvi et al., 2004).

Current technologies used for processing laterites include pyrometallurgical (e.g. ferronickel and matte smelting) and hydrometallurgical (e.g. high-pressure acid leaching) methods, and the hybrid Caron process, all of which require high energy and/or chemical consumption (McDonald et al., 2008). Heap leaching technologies are proposed as low energy

alternatives with less specificity on the mineralogy of the laterite but a longer duration period prior to steady state production (Oxley et al., 2016). Cobalt is generally present in one or two orders of magnitude less than nickel in laterites, and therefore not usually considered an economically viable source of this metal. Cobalt can also be found in waste materials generated by processing laterites, including tailings (Marrero et al., 2015) and processing residues (e.g. slags) where concentrations may be greater than in the primary ores.

Several studies have demonstrated that limonite ores and laterite tailings are amenable to bioprocessing by acidophilic bacteria at relatively low temperatures (Hallberg et al., 2011; Johnson and du Plessis, 2015; Marrero et al., 2015; Smith et al., 2017). The approach used has been described as 'biomining in reverse gear' and is mediated by many of the same acidophilic microorganisms that are also used in conventional biomining operations, but in set-ups engineered to facilitate iron reduction rather (as in conventional biomining) iron oxidation. When processing oxidised ores, such as laterites, it is necessary to add an extraneous source of energy for the bacteria in order to provide an electron donor that can be coupled to iron reduction. Both organic and inorganic electron donors can be used, though zero-valent sulfur (ZVS) has been the material of choice, both because of its low cost and the fact that its oxidation, coupled to oxygen or soluble iron (III), generates sulfuric acid which helps to maintain the acidic conditions that enhance both metal dissolution and the activities of the acidophilic microorganisms.

Lateritic ores have the potential to become major sources of cobalt in the future, and developing more environmentally benign technologies for processing these materials is an urgent issue. This work, carried out as part of the EU-funded CROCODILE project (https://h2020-crocodile.eu/), describes results from bioprocessing different oxidised cobalt-bearing materials, including three primary limonitic laterite ores from different mines in Greece, and two processing residues. The materials were all bioleached by a consortium of acidophilic bacteria in stirred tank bioreactors.

2. Material and methods

2.1. Sample characterisation

Five cobalt-bearing materials were bioprocessed at low pH and mesophilic temperatures (Table 1). All samples were provided by LARCO (General Mining and Metallurgical Company SA, Larymna, Greece), a partner in the EU-funded CROCODILE project. Three of these materials were limonitic ores from different mining operations in northern and central Greece, and the other two, a slag and a black filter dust, were wastes generated at a smelting plant for ferronickel production. Sample L1 was a very fine-grained black dust and L2 a crushed, black porous slag with occasional small (<500 μm) metallic beads. The Kastoria (sample L3) limonite zone forms the upper part of an *in situ* laterite deposit, whilst at Agios Ioannis (sample L4) and Evia (sample L5), the deposits are reworked karstic types, dominated by oxides with the Agios Ioannis limonite developed below a bauxitic laterite (Herrington et al., 2016). The three limonite samples were ground using a disc mill with a 500 μm disc separation, homogenised and sieved to <900 μm. Mineralogical and chemical analyses of samples and bioleached residues were carried out using a combination of techniques, including induction coupled plasma atomic emission spectroscopy (ICP-AES), induction coupled plasma mass spectrometry (ICP-MS), X-ray powder diffraction (XRD; PANalytical X'Pert Pro α1 scanning diffractometer) and thermogravimetry/differential thermal analysis (TG-DTA; TA Instruments SDT Q600). Detailed characterisation of cobalt hosting mineral phases was performed using scanning electron microscopy (SEM; Zeiss EVO 15LS SEM) and electron probe micro analyser (EPMA; Cameca SX100).

2.2. Bacterial cultures

A mixed culture consortium of acidophilic iron-oxidizing/reducing and sulfur-oxidizing bacteria were used in experimental work. The consortium contained *Acidithiobacillus* (*At.*) *ferrooxidans*^{T} and *At. ferrooxidans* strain CF3, *At. ferriphilus*^{T}, *At. ferridurans*^{T}, *Sulfobacillus*

(*Sb.*) *thermosulfidooxidans*^{T}. All cultures were sourced from the *Acidophile Culture Collection* maintained at Bangor University. A starter culture of the consortium was set up in shake flask containing 100 mL of liquid medium, containing basal salts and trace elements (Ñancucheo et al., 2016), 100 µM ferrous sulfate and 5% (w/v) ZVS at pH 2.5, and incubated at 35°C in an orbital shaker.

2.3. Reductive bioleaching experimental set up

Bioreactor vessels (2 L working volume) coupled to FerMac 300 modular units that controlled pH, temperature and agitation (Electrolab, UK) were commissioned for each experiment, each using one of the five cobalt-bearing materials. Liquid medium containing basal salts and trace elements was added to each reactor vessel, followed by 1% (w/v) ZVS. All reactors were heat-sterilised at 110°C for 60 min and ferrous sulfate (100 µM) and 100 mL of the starter culture were added to the reactor, when cool. The pH in the bioreactors was maintained at 1.5 by automated addition of 1 M H_2SO_4 or 1 M NaOH and temperature fixed at 35°C. All reactors were stirred at 150 rpm. The bioreactors were initially aerated with sterile atmospheric air in order to promote biomass growth using ZVS as the electron donor coupled to the reduction of molecular oxygen. Seven to ten days after the bioreactor inoculation, the gas supply was switched to oxygen-free nitrogen (OFN) to generate anaerobic conditions. Each cobalt-bearing material was added to the bioreactors at 5% (w/v) solid load. Volumes of acid or alkali consumed in order to maintain the pH of the bioreactor at 1.5 were recorded and cumulated daily. Liquid samples were withdrawn at regular intervals, pH and redox potential measured off-line, and metals concentration determined. Reductive bioleaching of the five samples was carried out for 25 - 30 days. At the end of each experiment, the solid phase was separated from the liquid phase (pregnant leaching solution; PLS) by filtration through Whatman (UK) #1 filter papers. The PLS was stored at 4 - 10ºC, and solid residues dried at room temperature, ground to fine powders using a pestle and mortar, and analysed for their mineralogical and geochemical compositions.

150 *2.4. Analytical techniques*

151

152 Concentrations of soluble iron (II) were determined using the Ferrozine assay
153 (Stookey, 1970). To measure concentrations of total soluble iron, an excess of ascorbic acid
154 was used in order to reduce soluble iron (III) to iron (II) and the resulting solutions analysed
155 again using the Ferrozine reagent. Concentrations of transition metals in leachates were
156 measured using a SpectrAA Duo atomic absorption spectrophotometer (Varian, UK). pH
157 values were measured using a pHase combination glass electrode (VWR, UK) and redox
158 potentials measurements using a platinum/silver-silver chloride electrode (Thermo Scientific,
159 UK) and were adjusted to be relative to a standard hydrogen electrode (i.e. E_h values). Both
160 electrodes were coupled to an Accumet 50 pH meter.

161

162 *2.5. Biomolecular analysis*

163

164 The compositions of the bacterial communities of the different PLS produced were
165 determined at the end of each experiment. Samples were filtered through sterile 0.2 µm (pore
166 size) membrane filters to collect biomass and DNA extracted using DNeasy PowerSoil Kit
167 (Qiagen, UK). Bacterial 16S rRNA genes were amplified and analysed using terminal
168 restriction enzyme fragment length polymorphism (T-RFLP), as described by Santos and
169 Johnson (2017). Terminal restriction enzyme fragments (T-RFs) were separated by capillary
170 electrophoresis and their lengths and fluorescence intensity were measured using a Beckman
171 Coulter CEQ8000 Genetic Analysis System and identified by comparison to the database of
172 acidophilic microorganisms maintained at Bangor University.

173

174 **3. Results**

175 *3.1. Characterisation of the cobalt-bearing materials*

176

177 Mineralogical analysis showed that the filter dust (L1) was dominated by quartz and a
178 spinel (magnetite), and also contained silicates, phyllosilicates and clay minerals, while calcite
179 ($CaCO_3$) was identified as a minor phase. The processed slag (L2) was essentially an
180 amorphous glassy phase with traces of maghemite and olivine (Table 2).

181 Quartz occurred as a major mineral phase in all three limonite ore samples. Goethite,
182 serpentine and calcite were also identified as major phases in sample L3, which additionally
183 contained hematite and low amounts of phyllosilicate and clay minerals. In sample L4 both
184 goethite and hematite were abundant phases, and phyllosilicates including clay minerals were
185 found in trace amounts. In sample L5, hydrated hematite was identified as the main iron (III)
186 oxide phase rather than goethite. Chlorite, smectite and serpentine were also present and,
187 unlike the other laterites, it also contained two carbonate minerals, calcite and ankerite
188 ($Ca(Fe,Mg,Mn)(CO_3)_2$) the latter in low abundance.

189 The chemical composition of the samples is shown in Table 3. The processing residues
190 (samples L1 and L2) consisted predominantly of silicon and iron. The slag (L2) had more iron
191 than the dust (L1) but contained an order of magnitude less nickel. Laterite samples L3, L4
192 and L5 had similar concentrations of silicon to each other. Sample L4 contained ~ 350 g kg^{-1}
193 iron which was almost twice as much as L3. Sample L4 contained very low levels of calcium
194 compared to L3 and L5, but concentrations of aluminium, vanadium and chromium were
195 greater. Sample L3 differed from both L4 and L5 in containing ~3 to 4-times more magnesium,
196 having a very low aluminium content and the lowest concentration of chromium of all three
197 laterites. Concentrations of nickel were similar in L3 and L4, but were much smaller (~50%
198 less) in L5. The filter dust (L1) had the highest concentration of cobalt, and the slag (L2) the
199 lowest, of the five samples tested.

200 In the filter dust (L1) and all laterite samples (L3, L4 and L5) cobalt was associated
201 mainly with manganese within lithiophorite-asbolane intermediate Mn-oxyhydroxides. This
202 mineral was found to contain between 0.79 and 9.47 wt% of Co (average value Co 3.21 wt%).
203 Cobalt was also present in goethite in samples L3 and L4 (0.03 to 0.27 wt%, average value
204 0.04 wt%), in the smectite of L5 (most likely nontronite 0.03 to 0.13 wt%, average value 0.08

wt%), in manganese carbonate (L3 only; 0.03 to 0.27 wt%, average value 0.15 wt%) and in chromites (0.03 wt% to 0.15 wt%, average value 0.06 wt%). Manganese carbonate and chromite were present in these samples in very low abundances, below the detection limit of XRD, but were observed in SEM and EPMA.

3.2. Sulfur-enhanced reductive bioleaching

The consortium of acidophilic iron-oxidising bacteria used in bioreactor experiments, was able to couple the oxidation of ZVS to the reduction of iron (III) under anaerobic conditions. The reductive dissolution of iron (III) (hydroxy)-oxide minerals was accompanied by increasing concentrations of soluble (ferrous) iron and other metals (Fig. 1).

Cobalt was effectively leached from all five Co-bearing materials. A rapid increase in cobalt dissolution occurred in the first 48 hours, followed by a slower phase of continuous dissolution (Fig. 1a). The kinetic data suggest that more protracted leaching would have enabled greater extraction of both cobalt and nickel for most of the samples tested (Figs. 1a and 1b). Manganese solubilisation followed a similar trend to that of cobalt, with the exception of the filter dust sample L1 (Fig. 1c). Concentrations of soluble manganese were highly correlated with those of cobalt, with regression coefficients >0.90, again with the exception of sample L1 where the value was 0.86. Data of nickel and iron extraction from the Co-bearing materials are shown in Fig 1b and 1d, respectively. Concentrations of nickel in the PLS ranged from 150 mg L^{-1} for L4 to 390 mg L^{-1} for L2. Iron solubilisation also varied greatly, with the smallest concentration of 400 mg L^{-1} total soluble iron for L4 and the largest (9,400 mg L^{-1}) for the slag (L2). There was a strong correlation between iron and nickel solubilised (R^2 > 0.90) for all laterite ores, but the values were lower (~ 0.80) for both processing residues.

By inducing anaerobic conditions, a major change in solution chemistry occurred, from one dominated by iron (III) to one dominated by iron (II), though this was more protracted with limonite sample L4. In most cases, over 80% of total soluble iron was present as iron (II) in less than 24 hours after gassing with OFN, though with sample L4 this figure was not reached

until day 20 (Fig. 2a). These changes were also reflected in redox potentials, as shown in Fig 2b. For limonite samples L3 and L5, E_h values sharply decreased (by ~ +100 mV) in the first 24 hours, stabilising at between +620 and +640 mV, but for sample L4, the fall in E_h was much slower, taking about 20 days to stabilise at ~ +620 mV. Redox potentials of PLS of both processing residues decreased to below +600 mV by day 2 and stabilised at +550 mV for L1 and ~ +400 mV for L2.

The reductive dissolution of iron (III) (hydroxy)oxides (shown for goethite in Eq. 1) is a proton-consuming reaction and addition of sulfuric acid was necessary to maintain solution pH at 1.5.

$$6FeO{\cdot}OH + 2S^0 + 10H^+ \rightarrow 6Fe^{2+} + SO_4^{2-} + 8H_2O \qquad \text{(Eq. 1)}$$

Cumulative acid consumption throughout each of the experiments is shown in Fig. 3. Sample L4 consumed far less acid (60 mmoles) than the other samples, which corresponded to this material containing only trace amounts of carbonate minerals and showing lower rates of iron dissolution. Samples L1, L3 and L5 consumed over 380 mmoles sulfuric acid to maintain pH at 1.5, while the slag waste (L2) consumed 730 mmoles.

Extraction of cobalt was similar with all five samples, with about 40 - 50% solubilised over the timescale of the experiments (Table 4). Dissolution of nickel varied greatly, with recoveries varying between 37% for L4 and 73% for L3. The extent of iron solubilisation from all of the limonite ores was less than that of both cobalt and nickel (and was only 2% for sample L4) but was considerably higher for both of the processing residues (Table 4).

In general, analysis of the solid phase bioleaching residues supported results obtained with the PLS, with the major discrepancies most likely due to the potential for heterogeneity and the very small sample volume analysed in the solid residue (Supplementary Table S1). XRD analysis showed that there had been some dissolution of ferric iron minerals, and residual ZVS was also detected in all residues (Fig. 4). In addition, gypsum precipitated in all samples except for L4, which had the lowest Ca content and did not contain detectable carbonates. Analysis of the bioleached filter dust (L1) residue revealed that there had been a

loss of magnetite, carbonate and a lower clay mineral content due to bioleaching. Carbonate (in L3 and L5) and serpentine were removed during low pH bioleaching of all the laterite samples and there were also lower clay contents in the bioleached residues. The removal of serpentine was most prominent in sample L3, where this phase was much more abundant than in samples L4 and L5. For the limonite samples, the strong correlation between cobalt and manganese suggested that cobalt was solubilised, predominantly, from manganese oxyhydroxide minerals. This was also confirmed by SEM investigation of the bioleaching residues, where it was observed that manganese-rich phases were no longer detected or were in a much lower abundance in the leached residues (Supplementary Fig. S1).

Bacterial diversities in the final PLS were much lower than that in the initial inocula. *At. ferrooxidans* and *Sb. thermosulfidooxidans* were detected in L3 leachate, while only *At. ferrooxidans* was detected at the end of bioleaching of L4 and L5 limonites. All attempts to amplify 16S rRNA genes from both L1 and L2 leachates were unsuccessful.

4. Discussion

The abundance of limonitic laterite ores in tropical and sub-tropical areas represent a large resource of cobalt yet to be exploited. Previous studies have shown that different primary target metals, including nickel (Johnson et al., 2013), copper (Ñancucheo et al., 2014) and cobalt (Smith et al., 2017) can be recovered from limonitic ores via reductive bioleaching. There have, however, been no previous reports of bioprocessing lateritic ores located in Europe, or none about using this approach to recover metals from ore processing wastes, with the exception of laterite tailings from the CARON process (Marrero et al., 2015). In addition, the comprehensive inventory of the detailed mineralogy of the three limonitic samples used in the present study illustrate how variations between lateritic ores, even within the same geographical location, can impact their amenability for bioleaching.

The smelting operation at Larymna (Greece) generates different solid waste materials, one being a fine dust which is collected in filters during the process of ferronickel production,

289 which contained greater concentrations of cobalt and nickel than in the limonite ores tested
290 (Table 3). Smelting of ore in an electric furnace at the Larymna site produces a metallic phase,
291 which contains most of the nickel, and a slag phase, which accounts for 85% of the furnace
292 feed. These are separated; the former is further processed, and the latter is mostly discarded.
293 In contrast to the filter dust, the slag contained less cobalt and nickel than the limonitic ores
294 tested. The three limonites, sourced from different mines in Greece, showed significant
295 variability in elemental and mineralogical composition.

296 Iron (III) minerals are known to be highly variable in terms of their susceptibility for
297 reductive dissolution at low pH (Bridge and Johnson, 2000). The mechanism by which
298 acidophilic prokaryotes accelerate the dissolution of iron (III) minerals is thought to be by
299 reducing small amounts of soluble iron (III) produced by the acid dissolution of these minerals,
300 shifting the equilibrium between iron (III) present in the solid and soluble phases (Johnson and
301 du Plessis, 2015). The rate-limiting step is usually the abiotic acid dissolution of the mineral
302 with, for example, goethite being much more susceptible than hematite. Acidophilic bacteria
303 that couple the oxidation of ZVS to the reduction of iron (III) can, however, also oxidise iron
304 (II) when oxygen is present, so anaerobic conditions are usually required for reductive mineral
305 bioprocessing to occur. The reduction of iron (III) has also been observed in aerobic cultures
306 of acidophiles, such as *Acidithiobacillus caldus* and *Acidithiobacillus thiooxidans*, that do not
307 oxidise iron (Johnson et al., 2017), but the mechanism by which this happens is unknown, and
308 these bacteria do not grow *via* iron respiration. The reductive dissolution of iron (III) and
309 manganese (IV) oxyhydroxide minerals, such as goethite and lithiophorite-asbolane, is highly
310 consumptive of protons (hydronium ions) which is why addition of sulfuric acid was required
311 to maintain the pH of all bioreactors. The presence of calcite and other basic minerals (e.g.
312 serpentine, chlorite) also contributed to the net acid consumption, which is a significant cost
313 associated with reductive mineral bioprocessing (Johnson and du Plessis, 2015). It was
314 interesting to note that the three limonite samples varied greatly in acid demand, with limonite
315 sample L4 requiring ~ 10 - 15 times less acid to extract ~ 1.5 fold more cobalt than the other
316 two samples. Sample L4 required 3 moles H_2SO_4 g^{-1} cobalt extracted, compared with 18 moles

317 g^{-1} for L1, 67 moles g^{-1} for L2, 48 moles g^{-1} for L3 and 28 moles g^{-1} for L5. Acid consumption
318 was greater for the slag (L2) than all other samples tested, whereas the filter dust (L1) required
319 less acid to maintain the bioreactor pH than the slag and two of the limonites. The amount of
320 iron solubilised and acid consumed were highly correlated (R^2 >0.92) for all samples tested,
321 apart from limonite L4, providing strong supportive evidence that the reductive dissolution of
322 iron (III) (hydroxy)oxides, as well as the destruction of carbonates and other acid-soluble
323 minerals, was a major cause of acid consumption. Although the percentages of iron solubilised
324 from all three limonites were relatively small compared to the percentage of the other transition
325 metals leached, the large contents of iron (III) minerals in the ores meant that concentrations
326 of iron (II) in PLS were always greater than those of manganese (II).

327 The strong correlation between cobalt and manganese in the limonite leachates (R^2
328 >0.90) and in the bioleached mineral residues were in agreement with the finding that most of
329 the cobalt present was associated with manganese (IV) minerals rather than with iron (III)
330 minerals. Manganese oxyhydroxides can be solubilised either indirectly by microbially-
331 generated ferrous iron or directly by some species of acidophilic bacteria (Ehrlich, 2008). While
332 the objective in this study was to optimise cobalt extraction rather than nickel, the economics
333 of the process would ultimately be dictated more by nickel than cobalt yields, since the former
334 (currently the lower value metal) was present in orders of magnitude greater than the latter in
335 all samples apart from the slag (L2).

336 The results from this study highlight the importance of mineralogical variability in
337 dictating the amenabilities of different limonites to reductive bioprocessing. Combined
338 mineralogical and elemental analysis showed that goethite was the most abundant iron (III)
339 mineral in sample L3, while L5 was dominated by hematite and L4 contained a mixture of the
340 two minerals. Given the relative susceptibilities of the two iron (III) minerals to acid dissolution,
341 it might have been anticipated that the concentration of soluble iron in L5 would have been
342 less than in both L3 and L4 PLS, but this was not the case. In support of these data, a simple
343 acid leaching test (1 g of each of the limonite samples leached with 10 mL of 1 M sulfuric acid,
344 shaken at 30°C for 1 hour) generated concentrations of total soluble iron that followed a similar

trend of that obtained in the bioreactors, with more iron being released from L5 (~ 350 mg L^{-1}) than L3 (~ 200 mg L^{-1}), and both of these were orders of magnitude greater than L4 (4 mg L^{-1}). EPMA analysis suggested that the hematite in L5 was partly hydrated and this altered-type hematite may be the reason for high amounts of iron being solubilised in this sample. Jang et al. (2007) demonstrated that hematite may get hydrated without structural transformation to its fully hydrated equivalent (e.g. goethite) and also showed that such hydrated hematite presented higher solubility compared to non-hydrated hematite.

Another apparent anomaly was the relatively low amount and percentage of iron bioleached from sample L4, which contained appreciable amounts of goethite in addition to some hematite, and the largest percentage of total iron. XRD analysis showed that the peaks for hematite were broad, suggesting poorer crystallinity of this mineral phase, though this is not unusual in such materials. In addition, the peak height ratios between goethite and hematite were similar before and after bioleaching, suggesting that neither of these two minerals were dissolved or changed preferentially to the other. Analysis of the bioleached residue supported the low recovery rates for iron obtained from L4 leachates. It is interesting to note that, although the redox potential in L4 leachates by the end of the experiment were similar to those reached with samples L3 and L5, the decrease in E_h values was far more protracted with L4. There were significant amounts of soluble iron (III) present in leachates for a large part of the experiment, and less manganese was also solubilised than from L3 and L5. This suggests a partial inhibition of the iron-reducing bacteria present, which would have in turn limited the rate of goethite dissolution by limiting the disequilibrium between soluble iron (III) and iron (II), which is thought to be the major driver in promoting the continued abiotic dissolution of iron (III) minerals in anaerobic conditions (Johnson and du Plessis, 2015). Concentrations of chromium and vanadium in L4 were greater than in samples L3 and L5. Both of these transition metals can occur as oxy-anions, which are, in general, far more toxic to bioleaching microorganisms than cationic transition metals, such as cobalt and nickel (Dopson et al., 2014). Encouragingly, the relatively small amount of iron dissolved from L4 did not seemingly impact yields of the chief target metal (cobalt), though less nickel was extracted

373 from this limonite than the other two samples. The much lower acid consumption and amount
374 of iron solubilised would both have economic benefits to a full-scale process. Iron
375 (hydroxy)oxides in the Larco laterite samples contained relatively small amounts (~0.9 wt%)
376 of nickel, and, in these samples, this metal was, like cobalt, more concentrated in the
377 manganese oxide phases and in addition also in some silicates (>2 wt% in serpentine in
378 sample L3).

379 Concentrations of both cobalt and nickel in the slag (L2) were the lowest of the
380 materials tested in this study, and large amounts of acid was consumed during reductive
381 dissolution, generating PLS that contained 5.5 mg L^{-1} cobalt and ~390 mg L^{-1} nickel. In
382 contrast, PLS generated from the dust sample (L1), contained the largest concentrations of
383 both of these metals of all five samples tested, though again had a large acid-demand (seven-
384 fold more than limonite L4) and generated PLS with similar cobalt but much greater nickel
385 concentrations. Despite the need for acid, results demonstrate that the filter dust, a waste
386 material in the processing plant, can be successfully processed *via* reductive dissolution, and
387 may be an attractive alternative source of cobalt and nickel at the Larymna processing plant.

388 The decrease in the microbial community diversity observed in all five experiments
389 could be due to different reasons, including: (i) some of the bacteria out competing others
390 during the oxidative phase of sulfur oxidation, (ii) lack of CO_2 provision during the bioleaching
391 stage, (iii) the consortium not being adapted to the different materials prior to bioprocessing
392 and (iv) the increase in concentration of potentially toxic metal oxyanions in the leachates.

393

394 **5. Conclusions**

395

396 This work has demonstrated the feasibility of bioleaching base metals from European
397 limonitic laterite ores and waste materials from their processing under acidic, relatively low
398 temperature, reducing conditions, using bacteria that couple the oxidation of zero-valent sulfur
399 to the reduction of iron (III). High acid demand is one of the more significant OPEX associated
400 with reductive mineral bioprocessing, and varied greatly between the five samples tested in

401 the present study. The comprehensive mineralogical analysis of the three limonitic laterite
402 samples revealed significant variations between the ores, and demonstrated that elemental
403 and mineralogical variabilities can impact their amenability for bioleaching.
404
405 **Acknowledgments**
406
407 This work was supported by the European Union's EU Framework Programme for Research
408 and Innovation Horizon 2020 (“CROCODILE”; grant number 776473). We are grateful for the
409 support of LARCO staff, particularly Anthimos Xenidis and Yannis Kontos, and of Anastasios
410 Kladis (Admiris).
411
412 **References**
413
414 Bridge, T.A.M. and Johnson, D.B., 2000. Reductive dissolution of ferric iron minerals by
415 *Acidiphilium* SJH. Geomicrobiol. J. 17, 193-206.
416 https://doi.org/10.1080/01490450050121161.
417
418 Dalvi, A.D., Bacon, W.G., Osborne, R.C., 2004. The past and future of nickel laterites. PDAC
419 2004 International Convention, Trade Show & Investors Exchange, 1-27.
420
421 Dopson, M., Ossandon, F.J., Lovgren, L., Holmes, D.S., 2014. Metal resistance or
422 tolerance? Acidophiles confront high metal loads via both abiotic and biotic mechanisms.
423 Front. Microbiol. 5, 157. https://doi.org/10.3389/fmicb.2014.00157.
424
425 Ehrlich, H.L., Newman, D.K., 2008. Geomicrobiology of manganese. In: Ehrlich, H.L.,
426 Newman, D.K. (eds.). Geomicrobiology. 5th edition. Boca Raton, FL: CRC Press. pp. 347-
427 420.
428
429 Hallberg, K.B., Grail, B.M., du Plessis, C.A., Johnson, D.B., 2011. Reductive dissolution of
430 ferric iron minerals: a new approach for bio-processing nickel laterites. Miner. Eng. 24, 620-
431 624. https://doi.org/10.1016/j.mineng.2010.09.005.
432
433 Herrington, R., Mondillo, N., Boni, M., Thorne, R., Tavlan, M., 2016. Bauxite and Nickel-
434 Cobalt Lateritic Deposits of the Tethyan Belt. In: Richards et al. (eds.), Economic Geology
435 Special Publication. 19, 249-387. https://doi.org/10.5382/SP.19.14.
436
437 Jang, J.H., Dempsey, B.A., Burgos, W.D., 2007. Solubility of Hematite Revisited: Effects of
438 Hydration. Environ. Sci. Technol. 41:21, 7303-7308. https://doi.org/10.1021/es070535t.
439
440 Johnson, D.B., du Plessis, C., 2015. Biomining in reverse gear: using bacteria to extract
441 metals from oxidized ores. Miner. Eng. 75, 2-5.
442 https://doi.org/10.1016/j.mineng.2014.09.024.

Johnson, D.B., Grail, B.M., Hallberg, K.B., 2013. A new direction for biomining: extraction of metals by reductive dissolution of oxidised ores. Minerals 3, 49-58. https://doi.org/10.3390/min3010049.

Johnson, D.B., Hedrich, S., Pakostova, E., 2017. Indirect redox transformations of iron, copper and chromium catalyzed by extremely acidophilic bacteria. Front. Microbiol. 8, 211. https://doi.org/10.3389/fmicb.2017.00211.

Lambiv Dzemua, G., Gleeson, S.A., Schofield, P.F., 2013. Mineralogical characterization of the Nkamouna Co–Mn laterite ore, southeast Cameroon. Miner. Deposita 48, 155-171. https://doi.org/10.1007/s00126-012-0426-3

Marrero, J., Coto, O., Goldman, S., Graupner, T., Schippers, A., 2015. Recovery of nickel and cobalt from laterite tailings by reductive dissolution under aerobic conditions using *Acidithiobacillus* species. Environ. Sci. Technol. 49, 6674-6682. https://doi.org/10.1021/acs.est.5b00944.

McDonald, R.G., Whittington, B.I., 2008. Atmospheric acid leaching of nickel laterites review. Part I. Sulphuric acid technologies. Hydrometallurgy 91, 35-55. https://doi.org/10.1016/j.hydromet.2007.11.009.

Ñancucheo, I., Grail, B.M., Hilario, F., du Plessis, C., Johnson, D.B., 2014. Extraction of copper from an oxidised (lateritic) ore using bacterially catalysed reductive dissolution. Appl. Microbiol. Biotechnol. 98, 6297-6305. https://doi.org/10.1007/s00253-014-5687-6.

Ñancucheo, I., Rowe, O.F., Hedrich, S., Johnson, D.B., 2016. Solid and liquid media for isolating and cultivating acidophilic and acid-tolerant sulfate-reducing bacteria. FEMS Microbiol. Lett. 363. http://dx.doi.org/10.1093/femsle/fnw083.

Oxley, A., Smith M.E., Caceres, O., 2016. Why heap leach nickel laterites? Miner. Eng. 88, 53-60. http://dx.doi.org/10.1016/j.mineng.2015.09.018.

Roberts, S. and Gunn, A.G. (2014) Cobalt. In: Gunn, G. (ed.) Critical Metals Handbook, Oxford, Wiley-Blackwell. https://doi.org/10.1002/9781118755341.ch6.

Santos, A.L., Johnson, D.B., 2017. The effects of temperature and pH on the kinetics of an acidophilic sulfidogenic bioreactor and indigenous microbial communities. Hydrometallurgy 168, 116-120. https://doi.org/10.1016/j.hydromet.2016.07.018.

Smith, S.L., Grail, B.M., Johnson, D.B., 2017. Reductive bioprocessing of cobalt-bearing limonitic laterites. Miner. Eng. 106, 86-90. http://dx.doi.org/10.1016/j.mineng.2016.09.009.

Stookey, L.L., 1970. Ferrozine - a new spectrophotometric reagent for iron. Anal. Chem. 42, 779-781. https://doi.org/10.1021/ac60289a016.

US Geological Survey, 2020. Mineral commodities summaries. http://pubs.usgs.gov/periodicals/mcs2020/mcs2020.pdf. (accessed 2 March 2020).

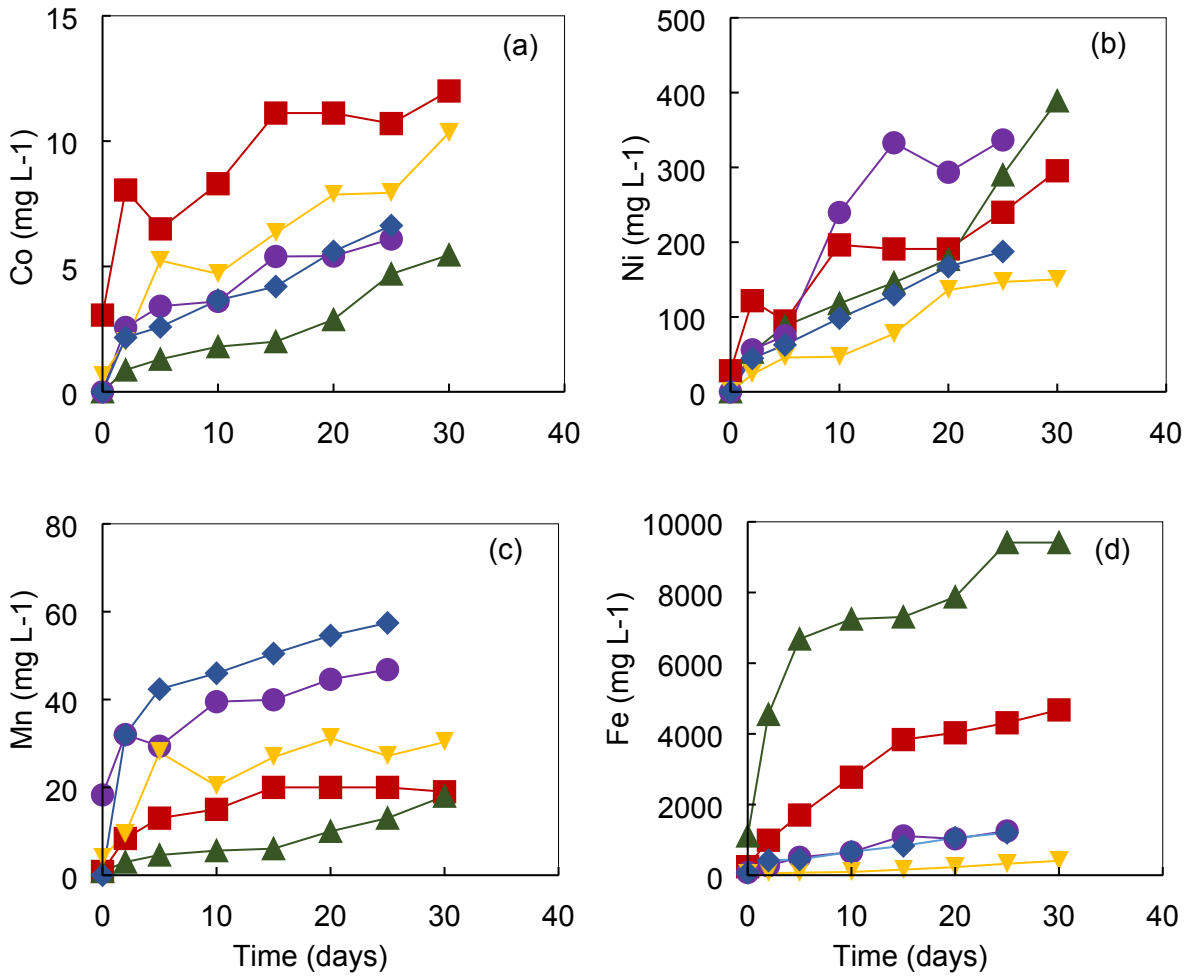

Figure 1. Changes in concentrations of soluble metals during bioprocessing of cobalt-bearing materials. Key: L1 (■); L2 (▲); L3 (●); L4 (▼); L5 (♦).

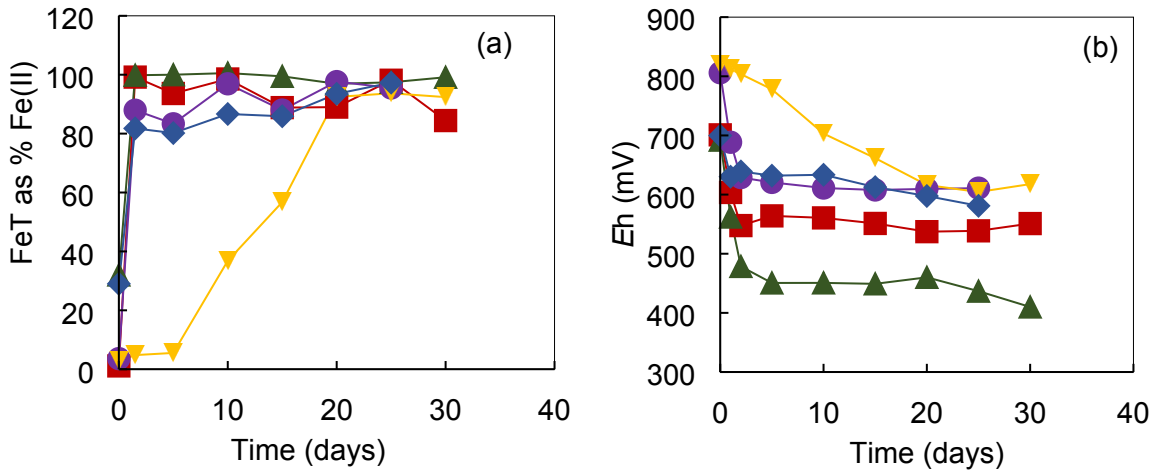

Figure 2. Changes in (a) concentrations of total soluble iron as a percentage of iron (II) and (b) redox potential values during reductive bioleaching of Co-bearing materials. Key: L1 (■); L2 (▲); L3 (●); L4 (▼) and L5 (♦).

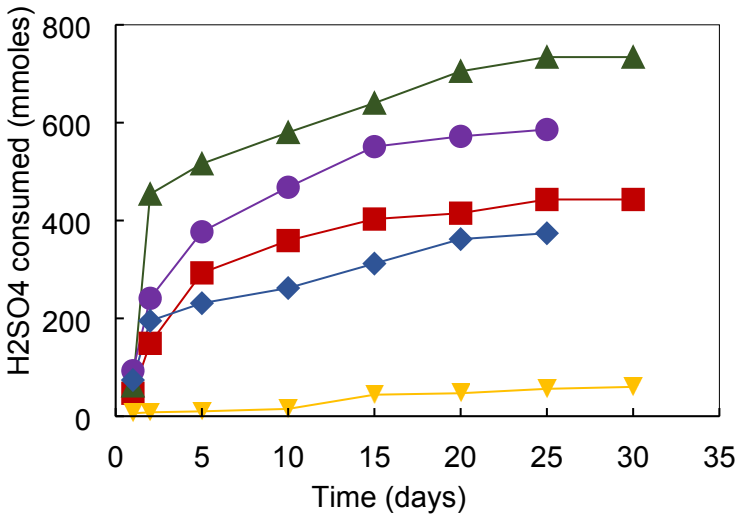

Figure 3. Cumulative amounts of sulfuric acid required to maintain bioreactors at pH 1.5 during bioprocessing of each Co-bearing material. Key: L1 (■); L2 (▲); L3 (●); L4 (▼) and L5 (♦).

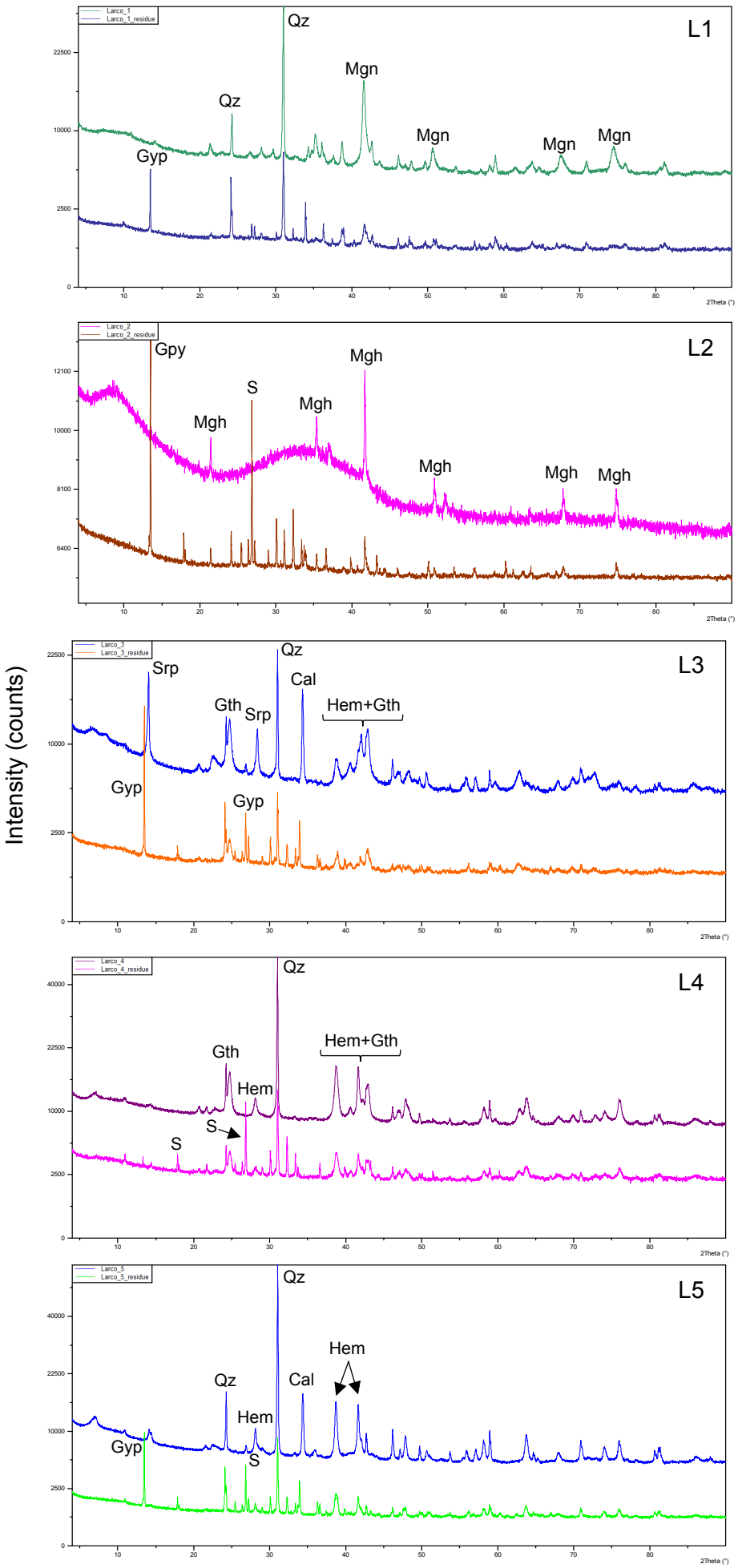
Intensity (counts)
L1
Larco_1
Larco_1_residue
Qz
Mgn
Qz
Mgn
Mgn
Mgn
Gyp
2Theta (°)
L2
Larco_2
Larco_2_residue
Gpy
Mgh
S
Mgh
Mgh
Mgh
Mgh
Mgh
2Theta (°)
L3
Larco_3
Larco_3_residue
Srp
Qz
Cal
Gth
Srp
Hem+Gth
Gyp
Gyp
2Theta (°)
L4
Larco_4
Larco_4_residue
Qz
Hem+Gth
Gth
Hem
S
S
2Theta (°)
L5
Larco_5
Larco_5_residue
Qz
Hem
Qz
Cal
Hem
Gyp
S
2Theta (°)

Figure 4. XRD patterns of the Larco samples before (upper pattern) and after (lower pattern) bioleaching. All leached residues had a lower intensity background indicating a reduction in total Fe concentration in the samples. Only the most prominent peaks on the patterns are labelled. Key: Qz-quartz; Mgn-magnetite; Gth-goethite; Mgh-maghemite; Hem-hematite; Cal-calcite; Gyp-gypsum; S-ZVS, Srp-serpentine.

Table 1. Summary of Co-bearing materials used in reductive bioleaching experiments.

Sample	Type of material	Location
L1	Filter dust	Larymna processing plant, Central Greece
L2	Processed slag	Larymna processing plant, Central Greece
L3	Limonite ore	Kastoria mine, Northern Greece
L4	Limonite ore	Agios Ioannis mine, Central Greece
L5	Limonite ore	Evia mine, Central Greece

Table 2. Mineral phases identified in bulk samples.

Sample	Mineral phases
L1	Quartz, hematite, magnetite, olivine, enstatite, calcite, serpentine, smectite, illite
L2	XRD-amorphous glassy material, maghemite, olivine
L3	Quartz, goethite, hematite, calcite, serpentine, talc, smectite, sepiolite
L4	Quartz, goethite, hematite, serpentine, chlorite, talc, smectite
L5	Quartz, hematite, calcite, ankerite, serpentine, chlorite, talc, smectite

Table 3. Concentration of selected elements in the cobalt-bearing materials. Filter dust (L1), slag (L2), limonite ore from Kastoria mine (L3), limonite ore from Agios Ioannis mine (L4) and limonite ore from Evia mine (L5).

	L1	L2	L3	L4	L5
Si*	169	192	143	126	169
Al*	38	34	5.2	29	21
Fe*	182	281	160	346	215
Ca*	36	32	42	2.3	57
Mg*	57	46	105	21	42
Cr*	14	21	6.8	18	10
Mn*	2.6	2.6	2.3	2.2	2.2
Ni*	11	1.1	10	8.2	5.6
Zn**	220	61	115	168	118
Cu**	44	18	17	38	23
V**	152	209	66	197	122
Li**	40	30	<10	10	40
Pb**	22	3	4	5	9
Sc**	34	44	19	47	24
Ba**	151	67	14	23	93
Co**	602	97	334	516	274

*g kg^{-1}; ** mg kg^{-1}

Table 4. Extraction of metals from limonite ores and processing residues (%) based on the chemical composition of the PLS.

Sample	Co	Ni	Mn	Fe
L1	41	53	15	48
L2	43	54	48	43
L3	39	73	44	17
L4	40	37	28	2
L5	49	68	52	12

Supplementary Table S1. Extraction of metals from limonite ores and processing residues (%) based on the chemical composition of the bioleached residues.

Sample	Co	Ni	Mn	Fe
L1	49	57	62	52
L2	25	10	48	43
L3	52	63	57	22
L4	47	38	39	4
L5	60	68	79	27

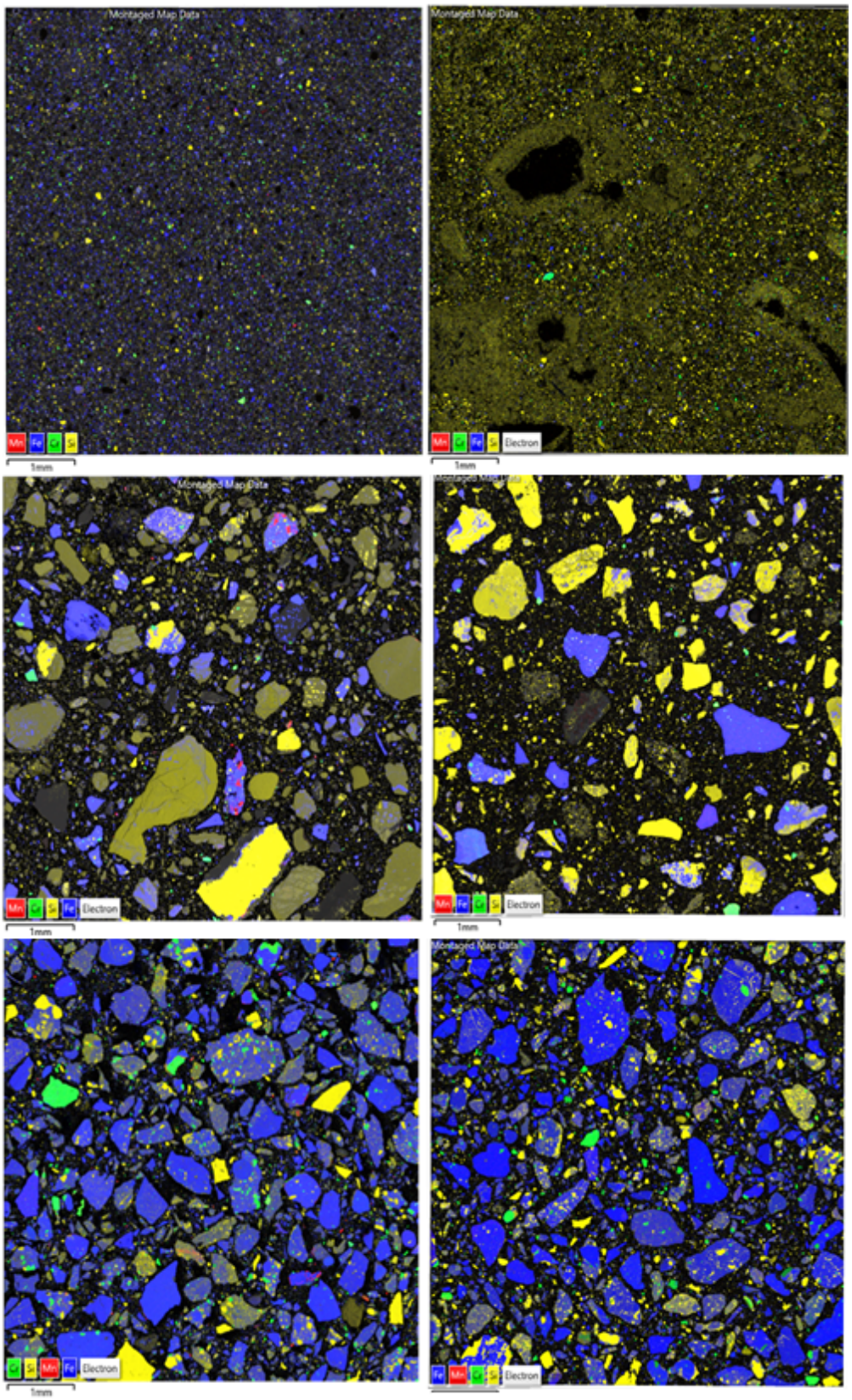

Supplementary Figure S1. SEM-EDX montaged maps showing distribution of manganese (red), iron (blue), chromium (green) and silicon (yellow) in Larco samples L1 (top), L3 (middle) and L4 (bottom) before (left panel) and after (right panel) bioleaching. Manganese oxy-hydroxides (in L1 and L4) and manganese carbonate (in L3) were identified in the samples before leaching as confirmed by EDX spectra extracted from all manganese-rich areas indicated on the maps of the unleached samples. Manganese was not detected in the samples after leaching.